JOURNAL OF VIROLOGY, Feb. 1994, p. 1040–1051
0022-538X/94/$04.00+0

Vol. 68, No. 2

Human Cytomegalovirus DNA Replicates after Early Circularization by Concatemer Formation, and Inversion Occurs within the Concatemer

MICHAEL A. McVOY* AND STUART P. ADLER

Departments of Pediatrics and Microbiology, Medical College of Virginia, Virginia Commonwealth University, Richmond, Virginia 23298

Received 12 July 1993/Accepted 4 November 1993

To determine the replicative mechanism for human cytomegalovirus (HCMV) DNA, field inversion gel electrophoresis was used to separate HCMV replicative DNAs during lytic infection. Unit-length circular HCMV genomes lacking terminal restriction fragments were detected starting 4 h after infection even when cells were treated with aphidicolin, phosphonoacetic acid, or cycloheximide. Viral DNA synthesis began 24 h after infection and produced large amounts of high-molecular-weight replicative DNA that was a precursor of progeny genomes. Replicative DNA contained rare terminal restriction fragments, and long-arm termini were much less frequent than short-arm termini. Replicative DNA was not composed of unit-length circles because low-dose γ irradiation of replicative DNA generated numerous random high-molecular-weight fragments rather than unit-length molecules. *Pac*I digestion of replicative DNA from a recombinant HCMV with two closely spaced *Pac*I sites revealed that replicative DNA is concatemeric and genome segment inversion occurs after concatemer synthesis. These results show that after circularization of the parental genome, DNA synthesis produces concatemers and genomic inversion occurs within concatemeric DNA. The results further suggest that concatemers acquire genomic termini during the cleavage/packaging process which preferentially inserts short-arm termini into empty capsids, causing a predominance of short-arm termini on the concatemer.

During lytic infection, the DNA of herpes simplex virus (HSV) and pseudorabies virus may replicate by a rolling circle mechanism following circularization of the linear viral genome, producing a concatemeric replicative intermediate (RI) (7, 26, 29). The evidence supporting a rolling circle mechanism for these viruses is that RI DNA sediments rapidly in sucrose gradients and is processed to make progeny genomes. The RI DNA lacks restriction fragments found at the genomic termini (terminal fragments) and fails to spread in electron micrographs (4, 5, 12, 17, 20, 31). In addition, early circularization has been inferred by a loss of terminal fragments shortly after infection, the appearance of novel fragments created by fusion of terminal fragments, and the occasional appearance of genome-length circular DNA in electron micrographs of DNA early after infection (6, 11, 12, 15, 19, 21, 28). Thus, for HSV and pseudorabies virus, all of the evidence is consistent with a rolling circle mechanism, but other replicative mechanisms are possible. For example, θ replication can produce a catenane of interlocked circular genomes which would have a high apparent molecular weight and lack terminal restriction fragments. Except for detection of some longer than unit length molecules by electron microscopy of HSV (12, 15, 18) and pseudorabies virus (4, 19) DNAs, the data do not exclude a circular structure for RI DNA (25, 30).

The human cytomegalovirus (HCMV) genome has a long and a short arm, each bordered by two different inverted repeat sequences called *b* and *c* (34). A short *a* sequence is found in multiple repeats of the same (direct) orientation at a region called the joint, where the two arms meet (35). Cleavage of replicative DNA occurs within *a* sequence repeats (33), leaving a variable number of *a* sequence copies at the long-arm terminus and a single or no *a* sequence at the short-arm terminus (36). The *a* sequence repeats remaining at the joint are not cleaved, apparently because of a "head full" requirement of the cleavage/packaging machinery (30). During infection, recombination allows both arms to invert relative to each other, resulting in equimolar amounts of four isomeric forms (34). Although the cleavage site (33) and an origin of replication (3, 10) and have been identified for HCMV, nothing is known about the mechanism of DNA replication. Therefore, we sought to characterize the macromolecular events occurring during replication of the HCMV genome.

* Corresponding author. Mailing address: Department of Pediatrics, Medical College of Virginia, Box 163 MCV Station, 1101 E. Marshall St., Richmond, VA 23298-0163. Phone: (804) 786-1808. Fax: (804) 371-6455.

MATERIALS AND METHODS

Viral culture and drug treatments. Confluent human MRC-5 fibroblasts (American Type Culture Collection) were infected with HCMV at a multiplicity of infection of between 1 and 5. Unless indicated otherwise, strain AD169 was used. Viral DNA was radiolabeled by propagation of infected cells in low-phosphate medium containing $^{32}P_i$ (50 μCi/ml), and labeled virus was isolated by centrifugation of cell-free culture supernatants at 35,000 × *g* for 1 h. In some experiments, cycloheximide (50 μg/ml), phosphonoacetic acid (PAA; 200 μg/ml), or aphidicolin (10 μg/ml) was added to the culture medium.

FIGE. Total cell DNA was prepared by washing infected cells with TE (10 mM Tris [pH 8.0], 1 mM EDTA), resuspending the cells in 50 μl of molten (50°C) 1% low-melting-point SeaPlaque agarose (FMC) in TE, and casting into molds. After cooling, agarose plugs were suspended in SE (0.5 M EDTA, 1% Sarkosyl, 1 mg of proteinase K per ml), incubated at 52°C for 48 h, dialyzed three times for 2 h each time with TE, and stored at 4°C. For preparation of virion DNA, extracellular culture supernatants were centrifuged at 35,000 × *g* for 1 h,

and the viral pellet was resuspended in agarose and treated as described above. Agarose blocks containing DNA were inserted into the loading wells of 1% SeaPlaque or SeaKem (FMC) agarose gels (11 by 14 cm) and separated by field inversion gel electrophoresis (FIGE) in 0.5× tris-borate electrophoresis buffer for 36 h at 120 V and 14°C. Pulse times began at 5 s and increased to 60 s with a forward-to-backward ratio of 3:1.

CHEF gel electrophoresis. Contour-clamped homogeneous electric field (CHEF) gel electrophoresis was carried out at 200 V for 30 h with a pulse time of 60 s and refrigeration set at 10°C in 1% SeaKem gels (14 by 14 cm) covered with 0.5× tris-borate buffer with a Pulsaphor CHEF apparatus (LKB).

Isolation of HCMV DNA forms by FIGE. HCMV-infected cell DNA was prepared as described above and separated by FIGE with SeaKem agarose for γ irradiation or with SeaPlaque for restriction enzyme digestion. For isolation of DNA that failed to migrate, agarose blocks that were inserted into the loading wells were removed following FIGE. For migrating DNA forms, markers consisting of HCMV-infected cell DNA prepared 7 days after infection were run flanking the samples of interest. Following FIGE, the marker lanes were cut from the gel, stained with ethidium bromide, and visualized with UV light. The locations of HCMV DNA in the marker lanes were then used to cut blocks of agarose containing the desired samples from the unstained portion of the gel.

DNA extraction and digestion. DNA for *Hin*dIII or *Eco*RI digestion was first extracted by GELase (Epicentre Technologies) digestion of SeaPlaque agarose followed by ethanol precipitation according to the manufacturer's instructions. In situ *Pac*I digestion of DNA in agarose was performed by dialysis in 1× NEB1 (New England Biolabs) buffer (three times for 30 min each time) and digestion in 50 μl of 1× buffer with 5 μl of *Pac*I (New England Biolabs) for 3 h at 37°C. Hirt isolation and $^{32}P_i$ labeling have been previously described (1, 2).

Southern transfer and hybridization. DNA separated either by FIGE or by conventional agarose electrophoresis was transferred to Nytran nylon membranes (Schleicher & Schuell) by capillary blotting, UV cross-linked (0.12 J/cm^2), and hybridized according to the manufacturer's instructions.

Plasmids. Plasmids were obtained from the following sources: HCMV Towne strain *Xba*I S and *Xba*I E fragments cloned in pACYC184, M. Stinski (University of Iowa, Iowa City); pON227 and pON2333, E. Mocarski (Stanford School of Medicine, Stanford, Calif.); pATH3ON, H. Brown (University of Cambridge, Cambridge, England); plasmid-cloned *Bam*HI W fragment of Epstein-Barr virus, J. Pagano (University of North Carolina, Chapel Hill); and pRSVZ, American Type Culture Collection. Probes were labeled with [^{32}P]dCTP (Amersham) by using a random hexamer priming kit (Boehringer Mannheim), and approximately 10^6 cpm was used per hybridization.

Nuclease sensitivity. Nuclease digestion was performed by a modification of the method of Lai and Chu (23). Infected cell monolayers were washed with phosphate-buffered saline, scraped, centrifuged, and resuspended in 150 μl of hypotonic buffer (10 mM Tris [pH 8.0], 12 mM KCl). After incubation on ice for 30 min, the lysate was homogenized 10 times in a tissue grinder and divided into 75-μl aliquots. To both samples were added 1.6 μl of 100 mM $CaCl_2$ and 8 μl of 10× nuclease buffer (600 mM KCl, 150 mM NaCl, 20 mM Tris [pH 7.8]). To the control sample, 3 μl of 0.5 M EDTA was added, and the tube was kept on ice to block the action of endogenous nucleases. To the treated sample, 1 μl (150 U) of *Staphylococcus aureus* nuclease (Boehringer Mannheim) was added, and digestion was carried out for 60 min at room temperature. Three microliters of 0.5 M EDTA was then added to stop the reaction, samples were embedded in 1% SeaPlaque agarose, and DNA was prepared as described above.

γ irradiation. DNA samples in agarose were suspended in 1 ml of TE in 1.5-ml microcentrifuge tubes and exposed to γ radiation, using a CES-I-RAD 1000 ^{137}Cs/^{134}Cs γ source.

Construction of MTO-1. The UL18 reading frame was selected as the insertion site because of its noncentral location within the long unique region. Plasmid pATH3O contains the *Hin*dIII O fragment of AD169 cloned into pAT153, and pATH3ON contains a synthetic polylinker inserted into the unique *Nde*I site within the UL18 reading frame. The polylinker was replaced with a unique *Pac*I site by *Nde*I digestion and linker insertion to yield pATH3OP.

Plasmid pRSVZ contains a β-galactosidase expression cassette consisting of the Rous sarcoma virus long terminal repeat linked to *Escherichia coli lacZ* (24). *Nde*I and *Apa*I restriction sites flanking the expression cassette were converted to *Pac*I sites by linker insertion to yield pRSVZP. pATH3OP was linearized by *Pac*I digestion, and the 5.3-kb *Pac*I fragment from pRSVZP containing the expression cassette was ligated to make pATH3OZ. *Hin*dIII-digested pATH3OZ was cotransfected with AD169 DNA into low-passage human foreskin fibroblasts, using a $CaPO_4$ transfection kit (Bethesda Research Laboratories). The LacZ$^+$ MTO-1 virus was isolated from the resulting virus stock by 5-bromo-4-chloro-3-indolyl-β-D-galactopyranoside (X-Gal) screening of infected 96-well cultures.

RESULTS

Identification of replicative forms of HCMV DNA. By using FIGE, four forms of HCMV DNA with different apparent molecular weights were detected between 3 h and 7 days after infection (Fig. 1A). At 3 h after infection, a 230-kb DNA appeared and increased in amount on day 3. At 24 h after infection, a high-molecular-weight (HMW) DNA that failed to migrate into the gel appeared and increased in amount 48 h after infection. Three days after infection, a 500-kb DNA and a 1,000-kb DNA appeared. When cells were separated into cytoplasmic and nuclear fractions 5 days after infection, all four forms were in the nuclear fraction and only 230-kb DNA was in the cytoplasmic fraction (experiment not shown).

HCMV DNA forms in the presence of PAA. To identify HCMV DNA forms found early in infection and in the absence of DNA synthesis, cells were infected in the presence of PAA. Prior to 48 h after infection, HCMV DNA forms observed in PAA-treated cells were identical to those in untreated cells (Fig. 1B). In contrast to untreated cells, 500- and 1,000-kb DNA forms were not observed. With PAA present, instead of increasing at 48 h, the amount of HMW DNA gradually decreased over time, indicating that the large quantities of HMW DNA observed in the absence of PAA are a product of the viral DNA polymerase (Fig. 1B). We call this DNA late HMW DNA. Even in the presence of PAA, however, some HMW DNA was detected at 24 h after infection. We call this DNA early HMW DNA.

Pulse-labeling of infected cell DNA. $^{32}P_i$ was added to the cell medium at various times after infection, and DNA samples were prepared after each pulse. Little ^{32}P incorporation occurred between 8 and 24 h after infection, but a significant increase in ^{32}P incorporation appeared in HMW DNA between 31 and 48 h after infection, and 1,000-, 500-, and 230-kb DNAs were labeled 55 h after infection (Fig. 2A).

Infected cells were also labeled between 24 and 48 h after infection and then washed and placed in medium containing

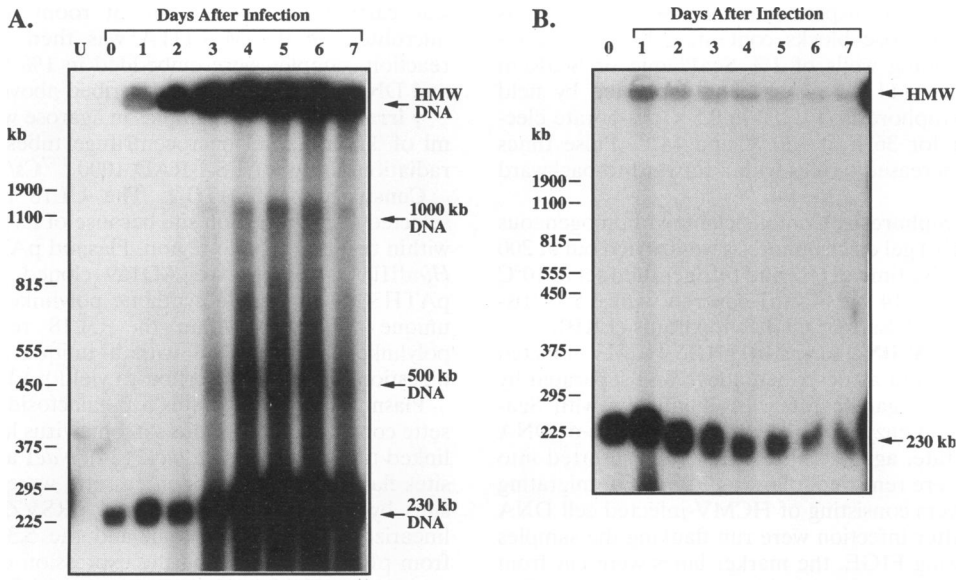

FIG. 1. HCMV DNA detected following FIGE separation and Southern hybridization with pON227 DNA. Day 0 was approximately 3 h after infection. (A) HCMV DNA in cells infected without PAA. (B) HCMV DNA in cells infected with PAA. Lane U contains uninfected cell DNA. Arrows indicate the migration positions of HCMV DNAs, and dashes on the left indicate the migration positions of yeast chromosomal markers.

unlabeled phosphate. DNA samples were prepared at various times after the chase. The 230-kb DNA was not detected at the end of the pulse (48 h) but appeared at 72 h and increased in amount until 117 h (Fig. 2B), indicating that 230-kb DNA is derived from one or more of the larger forms.

Nuclease sensitivity. To determine the HCMV DNA associated with capsids, cells at various times after infection were homogenized in hypotonic buffer and then treated with staphylococcal nuclease. At 3 h after infection, the 230-kb DNA was nuclease resistant (Fig. 3), but by 24 h after infection, most of this DNA was nuclease sensitive. The 230-kb DNA was again nuclease resistant 3 days after infection. HMW, 1,000-kb, and 500-kb DNAs were all nuclease sensitive, suggesting a lack of association with capsids.

Irradiation of late HMW and 1,000-kb DNAs. To detect circular DNA molecules, we used low-dose γ irradiation to randomly break double-stranded DNA. As a control, we irradiated Epstein-Barr virus circular episomes in Raji cells. Without irradiation, circular Epstein-Barr virus DNA did not migrate by FIGE, but with increasing doses of radiation, a 190-kb DNA was formed (Fig. 4A). In contrast, irradiation of HCMV HMW DNA from cells 5 days after infection produced a DNA smear of random-length fragments, indicating that HCMV HMW DNA is not composed of unit circles (Fig. 4B).

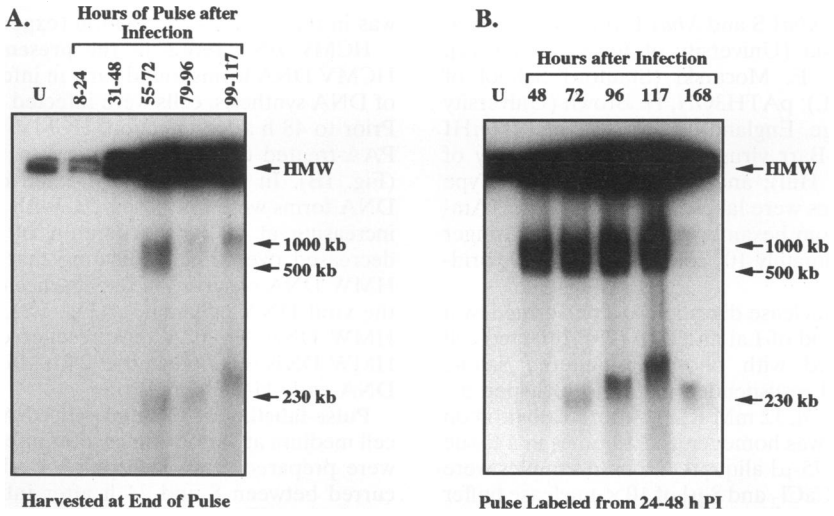

FIG. 2. Labeled HCMV DNA prepared from lytically infected cells and detected after FIGE separation by autoradiography of the dried gel. (A) Cells were pulse-labeled with $^{32}P_i$ when indicated, and DNA was prepared at the end of each pulse. Lane U contains DNA from uninfected cells prepared after 16 h of pulse-labeling. (B) Infected cultures were pulse-labeled from 24 to 48 h postinfection (PI) and then incubated with unlabeled phosphate. DNA was prepared when indicated. Lane U contains DNA from uninfected cells harvested after 24 h of pulse-labeling. Positions of the HCMV DNA forms are indicated.

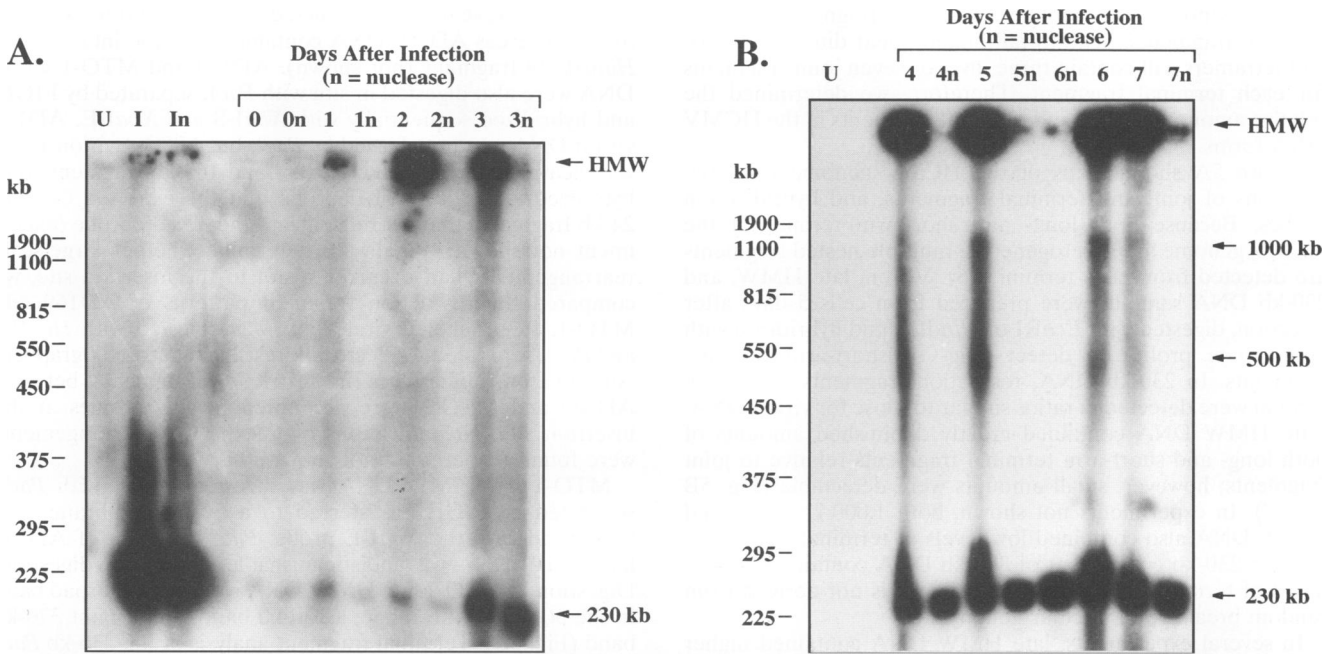

FIG. 3. Nuclease protection of HCMV DNA. Lysed infected cells were treated or mock treated with nuclease before DNA preparation. Following separation by FIGE, HCMV DNA was detected by Southern hybridization with labeled *Xba*I-E plasmid DNA. (A) Days 0 to 3, prolonged autoradiographic exposure. (B) Days 4 to 7, normal exposure. Lane U contains uninfected cell DNA, and lanes I contain viral inoculum DNA. The lanes marked n contain nuclease-treated samples. Positions of the HCMV DNA forms and yeast chromosomal markers are indicated.

Irradiation of 1,000-kb DNA also produced even smearing, indicating this form is not circular. Analysis of 500-kb DNA was not possible because this DNA consistently contained a 230-kb component even without irradiation (experiment not shown).

Terminal restriction fragment analysis of late HMW, 500-kb, and 1,000-kb DNAs. Because fusion of HCMV termini creates a sequence identical to the sequence at the joint region, restriction enzyme digests of circular genomes or head-to-tail concatemers will not contain novel restriction fragments. A

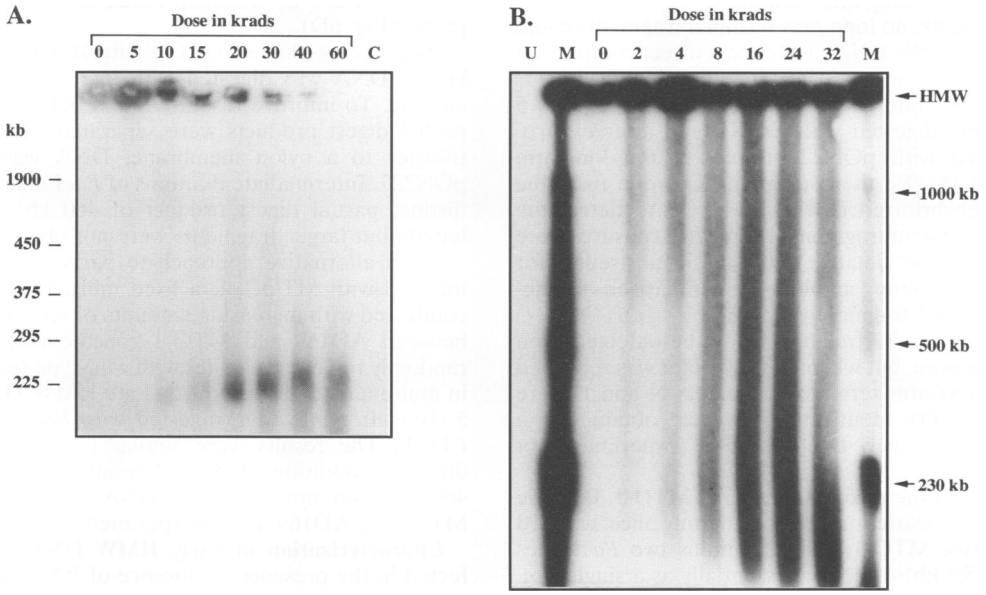

FIG. 4. Detection of the γ-irradiation products of HMW DNA. (A) γ irradiation of Raji cell DNA after FIGE separation and Southern hybridization with ^{32}P-labeled Epstein-Barr virus *Bam*HI-W plasmid DNA. Lane C is a negative control containing MRC-5 cell DNA 7 days after infection with HCMV. Positions of yeast chromosomal markers are indicated. (B) HCMV late HMW DNA was prepared from cells 5 days after infection, γ irradiated, separated by FIGE, and detected by Southern hybridization with labeled *Xba*I-E plasmid DNA. Lane U contains uninfected cell DNA, and lanes M contain HCMV-infected cell DNA prepared 7 days after infection.

circular genome will contain two joint fragments but no terminal fragments; head-to-tail-linked linear dimers, trimers, and tetramers will contain three, five, or seven joint fragments for each terminal fragment. Therefore, we determined the relative amounts of joint and terminal fragments in the HCMV DNA forms.

Figure 5A shows maps of the HCMV genome (34), the locations of joint and terminal fragments, and hybridization probes. Because both long- and short-arm termini of the HCMV genome are heterogeneous, multiple nested fragments are detected from both termini (36). Virion, late HMW, and 230-kb DNA samples were prepared from cells 5 days after infection, digested with *Eco*RI or *Hin*dIII, and hybridized with appropriate probes to detect long- or short-arm terminal fragments. In 230-kb DNA, restriction fragments from both termini were detected in ratios similar to those for virion DNA. Late HMW DNA contained greatly diminished amounts of both long- and short-arm terminal fragments relative to joint fragments; however, small amounts were detectable (Fig. 5B and C). In experiments not shown, both 1,000-kb DNA and 500-kb DNA also contained low levels of terminal fragments, and the 230-kb component of 500-kb DNA contained normal levels of terminal fragments, indicating it is not derived from random breakage of circular genomes.

In several experiments, late HMW DNA contained higher levels of short-arm terminal fragments than of long-arm terminal fragments. Using scanning densitometry of the experiment in Fig. 5 and a second similar experiment (not shown), we calculated the ratio of joint to terminal fragment quantities and divided this ratio by the ratio derived from virion DNA (the joint-to-terminus ratio of virion DNA is 1.00). As a control, ratios were determined for 230-kb DNA from cells 5 days after infection, and in two experiments, 230-kb DNA had ratios for both termini of approximately 1.00 (0.967 and 0.963 for the short-arm terminus; 0.676 and 0.987 for the long-arm terminus). Late HMW DNA had ratios of 14.8 and 16.3 for the short-arm terminus and 34.5 and 41.7 for the long-arm terminus. Thus, late HMW DNA contained roughly 2.5-fold more short-arm termini than long-arm termini.

In some experiments, no long-arm terminal fragments could be detected in late HMW DNA. To make a direct comparison between the levels of long- and short-arm terminal fragments in the same DNA sample, late HMW DNA was prepared 5 days after infection, digested with *Eco*RI, and after electrophoresis hybridized with pON227 to detect the long-arm terminal fragment W. We then stripped this probe from the membrane and rehybridized it with pON2333 to detect the short-arm *Eco*RI terminal fragments N and L. Exposures were adjusted to provide approximately the same signal strength for the joint fragments, enabling an objective comparison of long- and short-arm terminal fragment quantities.

No long-arm terminal W fragment could be detected even after extended exposure, but when the same blot was reprobed with pON2333, short-arm terminal fragments N and L were clearly visible (Fig. 5D). Identical results were obtained in a repeat experiment with new DNA samples (experiment not shown).

Characterization of the recombinant virus MTO-1. Because HCMV DNA lacks a restriction site present only once, we used a recombinant virus, MTO-1, which contains two *Pac*I sites sufficiently close (5.3 kb) to behave essentially as a single site. The predicted genome arrangement of MTO-1 and locations of hybridization probes are shown in Fig. 6A. This genome arrangement was confirmed by Southern hybridization both at the insertion site and on a genomic scale. Blots of MTO-1 DNA, digested with *Hin*dIII and *Pac*I and hybridized with pATH3OZ, revealed the predicted 2.3-, 5.3-, and 6.5-kb fragments, whereas AD169 DNA contained only the intact 8.7-kb *Hin*dIII O fragment (not shown). AD169 and MTO-1 virion DNA were also digested in situ with *Pac*I, separated by FIGE, and hybridized sequentially with *Xba*I-S and *Xba*I-E. AD169 virion DNA was not cleaved by *Pac*I, but MTO-1 virion DNA was cleaved into the expected 205- and 165-kb fragments that hybridzed with the *Xba*I-E probe and the expected 64- and 24-kb fragments that hybridized with the *Xba*I-S probe (experiment not shown). Finally, to determine whether large-scale rearrangements had occurred distal to the insertion site, we compared the restriction fragment patterns of AD169 and MTO-1. Pulse-labeled viral DNA was digested with *Hin*dIII and *Pac*I, separated by electrophoresis, and autoradiographed. All apparent differences in restriction fragments between AD169 and MTO-1 were accounted for by changes at the insertion site. No indications of unexpected rearrangements were found (experiment not shown).

MTO-1 late HMW DNA was digested in situ with *Pac*I, separated by FIGE, transferred to a nylon membrane, and hybridized with the *Xba*I-E probe. *Pac*I digestion of AD169 late HMW DNA was indistinguishable from mock digestion. Digestion of MTO-1 late HMW DNA resulted in a broad band in the 50- to 100-kb range, a 230-kb band, and a faint 370-kb band (Fig. 6B). Terminal fragment analysis of the 230-kb *Pac*I digest product revealed a lack of terminal fragments, confirming that this 230-kb DNA is not derived from contaminating genomic DNA (experiment not shown).

Figure 6C illustrates a model explaining the structure of the 370-kb fragment. If a concatemer is composed primarily of the prototype (P) isomer such that most *Pac*I sites are 230-kb apart, then occasional inversion of a P isomer to an inverted long-arm (I_L) isomer places the *Pac*I site of the I_L isomer 370 kb from that of the adjacent P isomer. The locations of hybridization probes predict that the *Xba*I-S probe will not hybridize with the 370-kb fragment. To test the model, the blot shown in Fig. 6B was stripped and rehybridized with the *Xba*I-S probe. Although the 230-kb fragment hybridized as before, the 370-kb fragment failed to hybridize to the *Xba*I-S probe (Fig. 6D).

Partial digestion of MTO-1 late HMW DNA. MTO-1 late HMW DNA was digested with increasing dilutions of *Pac*I enzyme. To improve resolution and obtain tighter bands, the partial digest products were separated by CHEF. Following transfer to a nylon membrane, DNA was hybridized with pON227. Intermediate dilutions of *Pac*I resulted in a faint but distinct partial digest product of 460 kb, or twice genome length, but larger fragments were not observed (Fig. 7).

In an alternative approach to partial digestion, cells were infected with MTO-1 at a fixed multiplicity of infection and coinfected with increasing amounts of AD169. Recombination between AD169 and MTO-1 concatemers was expected to randomly replace *Pac*I sites with wild-type sequences, resulting in multimeric digest products. Late HMW DNA was prepared 5 days after infection, digested with *Pac*I, and separated by CHEF. The results were similar to those seen for partial digestion: addition of AD169 resulted in a faint but distinct 460-kb band not visible in DNA from cells infected with MTO-1 or AD169 alone (experiment not shown).

Characterization of early HMW DNA. Cultures were infected in the presence or absence of PAA, and DNA samples were prepared at 4-h intervals. After FIGE separation and hybridization, the amounts of HMW DNA at each time point were compared between PAA-treated and untreated cultures. In the presence of PAA, a very small amount of early HMW DNA was detected at 4 h after infection and peaked in amount

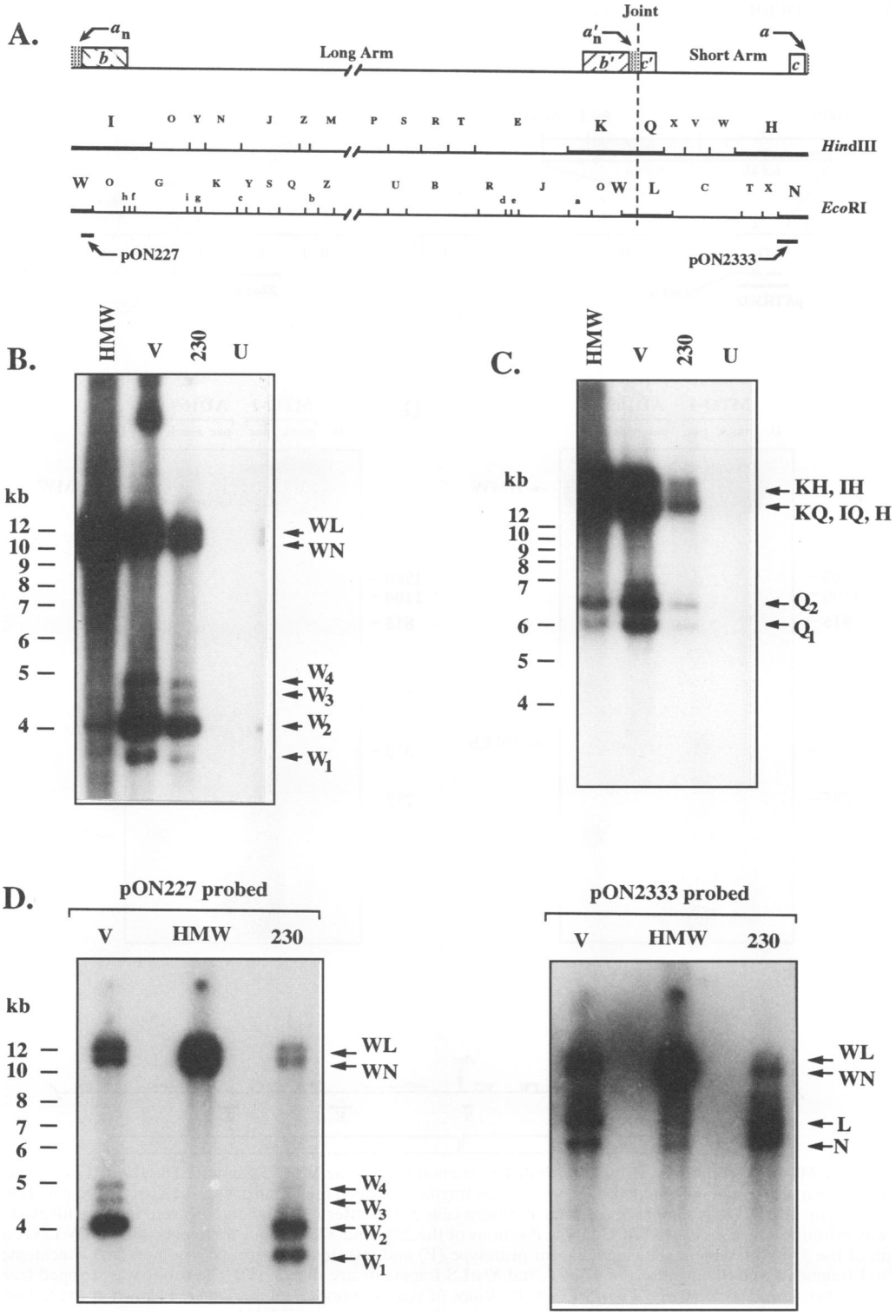

FIG. 5. Terminal fragment analysis of 230-kb and late HMW DNAs. (A) *Eco*RI and *Hin*dIII restriction maps of the HCMV strain AD169 prototype isomer showing the locations of terminal and joint fragments and plasmid-cloned fragments used as hybridization probes (boldface). Late HMW, 230-kb DNA, and virion DNA, all prepared from cells 5 days after infection, were digested with *Hin*dIII or *Eco*RI and electrophoresed on 0.6% agarose. (B) Hybridization of *Eco*RI digests with pON227 to detect long-arm terminal W fragments. Positions of molecular weight markers, W terminal fragments, and joint fragments WN and WL are indicated. Heterogeneous terminal fragments are numbered with subscripts beginning with the smallest fragment detected. Lane V contains virion DNA, and lane U contains uninfected cell DNA. (C) Hybridization of *Hin*dIII digests with pON2333 to detect short-arm terminal Q fragments. Positions of Q and H terminal fragments and joint fragments KQ, KH, IQ, and IH are indicated. (D) Comparison of long- and short-arm terminal fragments in late HMW DNA. *Eco*RI digests were prepared as described above, hybridized with pON227 to detect the long-arm terminal W fragments, stripped, and then reprobed with pON2333 to detect the short-arm terminal N and L fragments. The exposures were adjusted to produce equal signal strengths for the WN and WL joint fragments. Positions of the W, N, L, WN, and WL fragments and of molecular weight markers are indicated. Lane V contains virion DNA.

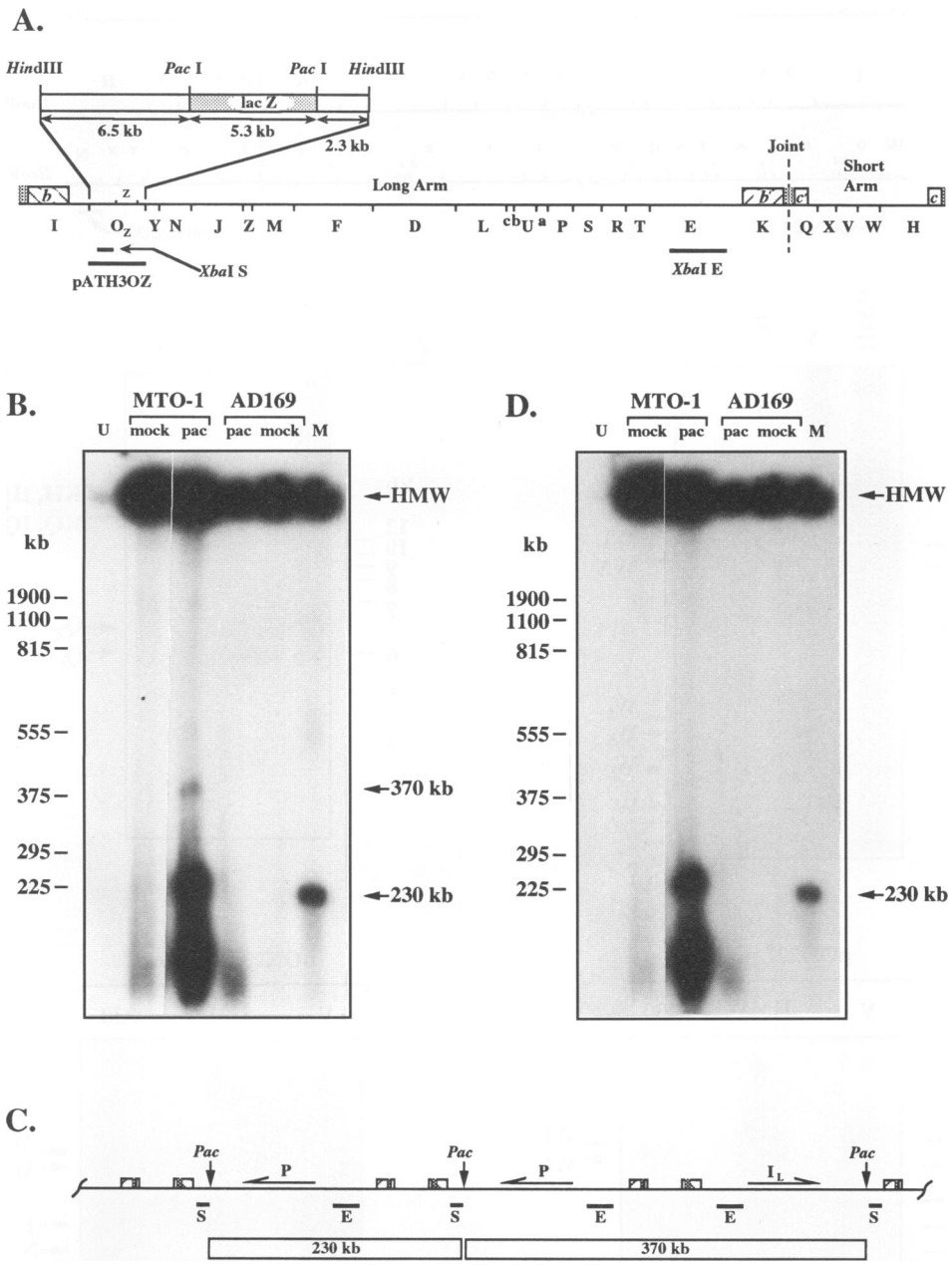

FIG. 6. Analysis of the MTO-1 recombinant virus. (A) *Hin*dIII restriction map of the MTO-1 genome. The *Hin*dIII O fragment containing the *lacZ* insertion has been renamed O_z and is expanded. The positions of fragments cloned in plasmids *Xba*I-E, *Xba*I-S, and pATH3OZ are indicated. (B) MTO-1 and AD169 late HMW DNA samples were prepared from cells 5 days after infection and digested in situ with *Pac*I. Following FIGE separation, DNA was hybridized with labeled *Xba*I-E DNA. Positions of the 230- and 370-kb *Pac*I fragments and HMW DNA are indicated. (C) Model of the origin of the 370-kb fragment showing adjacent prototype (P) and inverted long-arm (I_L) isomers in a concatemer. The predicted 230- and 370-kb *Pac*I fragments and the positions of *Xba*I-E and *Xba*I-S fragments are shown. (D) The probe was stripped from the nylon filter shown in panel B and rehybridized with labeled *Xba*I-S DNA. Positions of yeast chromosomal markers are shown at the left of panels B and D. Lanes M contain undigested infected cell marker DNA, and lanes U contain uninfected cell DNA.

between 12 and 16 h after infection. The first increase in HMW DNA in untreated cultures, compared with that of treated cultures, occurred between 20 and 24 h after infection and marked the beginning of late HMW DNA synthesis (Fig. 8).

Since the amount of early HMW DNA observed 24 h after infection is comparable to the amount of inoculum DNA observed 3 h after infection (Fig. 1B), it is possible that early HMW DNA is formed by a change in the structure of inoculum DNA. Cells were infected with virions containing ^{32}P-labeled genomes, and DNA was separated by FIGE. Labeled 230-kb DNA gradually diminished with time. The inoculum DNA was converted to an HMW form beginning at 6 h after infection (Fig. 9). Furthermore, neither aphidicolin nor cycloheximide affected the amount of early HMW DNA formed after infection (experiment not shown).

HMW DNA was prepared 24 h after infection from cultures

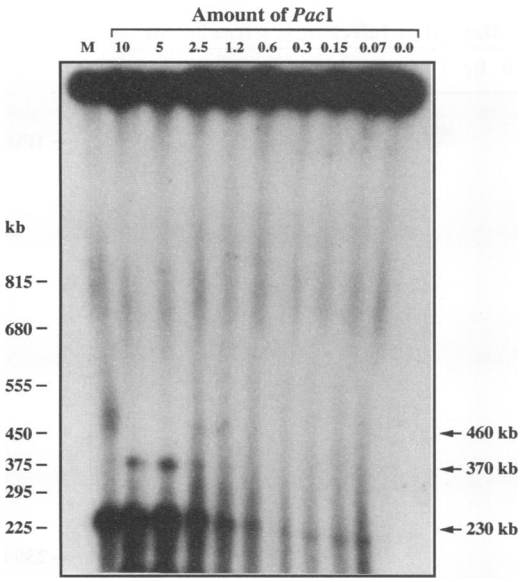

FIG. 7. Partial *Pac*I digestion of MTO-1 late HMW DNA. HMW DNA was prepared from MTO-1-infected cells 5 days after infection and digested in situ with the indicated amounts (microliters) of *Pac*I. Following CHEF gel electrophoresis, HCMV DNA was detected by Southern hybridization with labeled pON227 DNA. Migration positions of the 230-, 370-, and 460-kb *Pac*I digest products and of yeast chromosomal markers are indicated. Lane M contains undigested infected cell marker DNA.

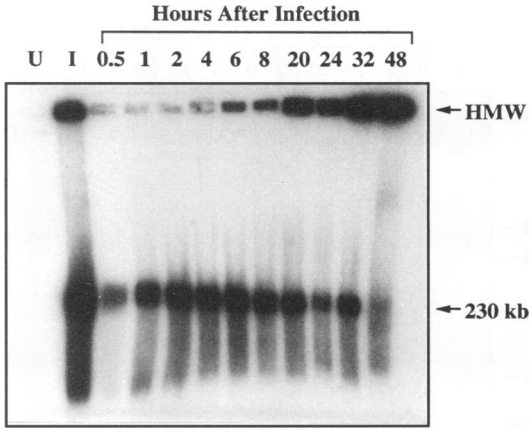

FIG. 9. Autoradiographs of FIGE-separated DNA prepared from cells infected with virions containing ^{32}P-labeled DNA. Lane U contains DNA from mock-infected cells, and lane I contains DNA from the labeled inoculum. Migration positions of 230-kb and HMW DNAs are indicated.

infected with or without cycloheximide, and replicate samples were exposed to increasing doses of γ radiation. In both cases, no 230-kb band was detected without irradiation, but increasing amounts of 230-kb DNA were observed after increasing doses of radiation (Fig. 10A). Similar results were obtained when DNA prepared after infection with PAA was used (experiment not shown).

Because circular DNA was not detected in late HMW DNA prepared 5 days after infection, we determined when after infection circular DNA molecules are no longer present. HMW DNA was prepared in duplicate samples daily after infection, and one sample was irradiated with 30 kilorads. Small amounts of 230-kb DNA were observed in irradiated samples at 24 and 48 h, but at later times after infection, smearing of large amounts of random-length fragments from late HMW DNA precluded the detection of small amounts of 230-kb DNA (Fig. 10B).

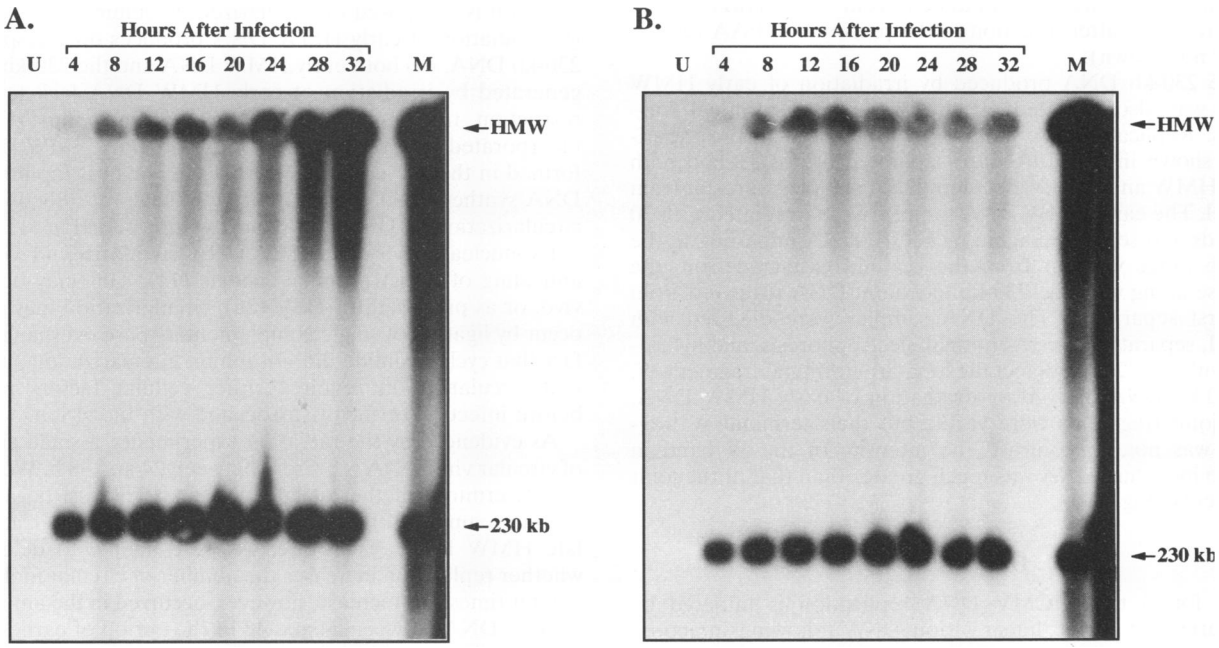

FIG. 8. Time course for the formation of early and late HMW DNA. Duplicate cultures were infected in the absence (A) or presence (B) of PAA, and DNA was prepared when indicated. Following FIGE, HCMV DNA was detected by Southern hybridization with labeled pON227 DNA. Lanes U contain uninfected cell DNA, and lanes M contain infected cell DNA 7 days after infection.

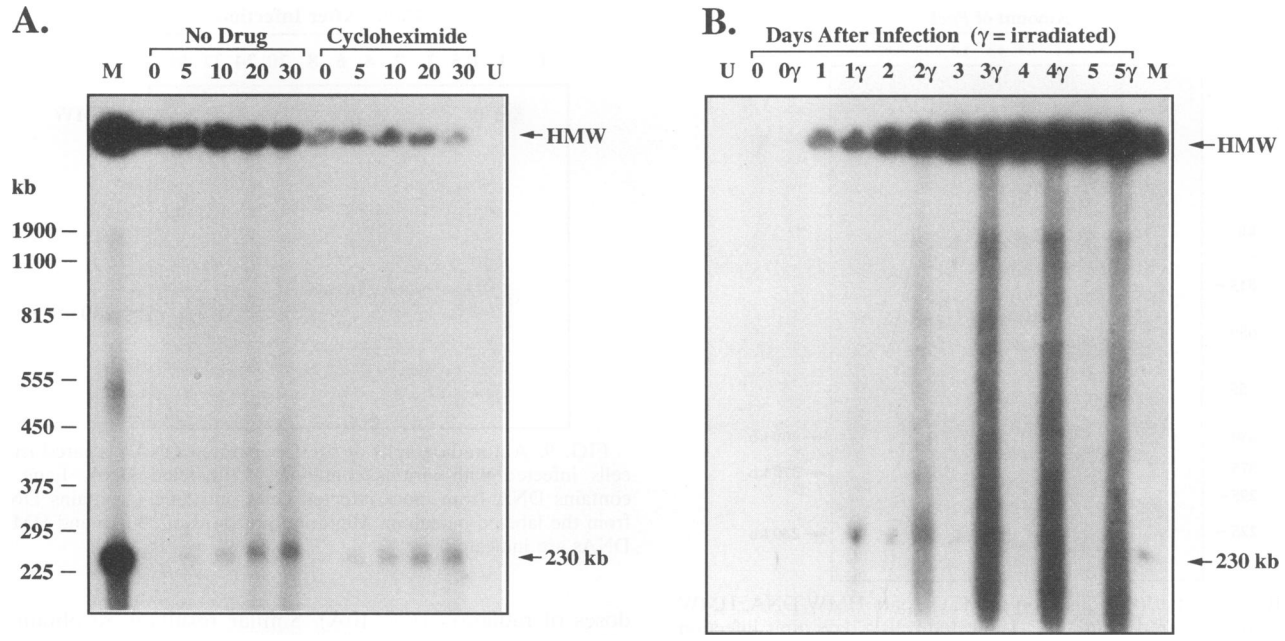

FIG. 10. Detection of irradiation products of HMW DNA early in infection. Following irradiation and FIGE separation, DNA was detected by Southern hybridization with labeled pON227 DNA. (A) Early HMW DNA was prepared from cells infected with or without cycloheximide and irradiated with the doses (kilorads) indicated. Lane U contains uninfected cell DNA irradiated with 30 kilorads, and lane M contains marker DNA prepared 7 days after infection. (B) Duplicate HMW DNA samples were prepared at the times indicated and either irradiated with 30 kilorads (γ) or mock irradiated. Lane U contains uninfected cell DNA irradiated with 30 kilorads, and lane M contains infected cell DNA 7 days after infection. Migration positions of the HCMV DNA forms and yeast chromosomal markers are indicated.

HMW DNA was prepared daily after infection and analyzed for the presence of terminal fragments. Late HMW DNA prepared 2 days after infection contained small amounts of short-arm terminal fragments and barely detectable amounts of long-arm terminal fragments. No terminal fragments were detectable in HMW DNA 24 h after infection (Fig. 11A and B). Similar results were obtained from early HMW DNA prepared 24 h after infection in the presence of PAA (experiment not shown).

The 230-kb DNA produced by irradiation of early HMW DNA was also analyzed for the presence of terminal fragments. Replicate DNA samples to those used in the experiment shown in Fig. 10A were separated by FIGE, and both early HMW and 230-kb inoculum DNA samples were cut from the gel. The early HMW DNA samples were irradiated with 30 kilorads and separated again by FIGE. DNA migrating in the 230-kb range was cut from the gel and extracted from the agarose along with the 230-kb inoculum DNA prepared from the first separation. The DNA samples were digested with *Eco*RI, separated by conventional electrophoresis, and hybridized with pON227 to detect the long-arm terminal fragment W. In 230-kb DNA derived by irradiation of early HMW DNA, both joint fragments were visible but their terminal W fragment was not. In contrast, the intensity of the W band in 230-kb inoculum DNA was much greater than that of the joint fragments (Fig. 11C).

DISCUSSION

We found that HCMV DNA replication is initiated by circularization of the linear virion DNA following infection. We first observed that at 3 h after infection, the 230-kb DNA present intracellularly is nuclease resistant with normal terminal fragments and therefore is most likely encapsidated inoculum DNA, but by 24 h after infection, nearly all of this 230-kb DNA is nuclease sensitive. At 3 days after infection, large quantities of encapsidated progeny genomes appear, and these genomes have a molecular size of 230 kb, have normal amounts of terminal fragments, and are nuclease resistant.

Early HMW DNA detected between 4 and 20 h after infection is composed of circularized inoculum DNA because (i) irradiation of early HMW DNA produces dose-responsive 230-kb DNA, (ii) both early HMW DNA and the 230-kb DNA generated by irradiation of early HMW DNA lack terminal restriction fragments, and (iii) labeled inoculum DNA is incorporated into early HMW DNA and early HMW DNA is formed in the presence of a viral (PAA) or host (aphidicolin) DNA synthesis inhibitor. Garber et al. have recently observed circularization of HSV DNA shortly after infection (13).

Exonuclease-treated HCMV DNA circularizes in vitro by annealing of direct terminal repeats (14). This may occur in vivo, or as proposed for HSV (26), circularization may simply occur by ligation of single complementary base overhangs. The fact that cycloheximide did not inhibit circularization suggests that circularization requires either cellular factors present before infection or factors associated with the virion.

As evidenced by the radiation experiments, a small amount of circular viral DNA is present between 24 and 48 h. We could not determine whether at later times circles exist because of the large amount of random fragments caused by irradiating late HMW DNA. Therefore, we were unable to determine whether replication increases the number of circular molecules at later times. No increase, however, occurred in the amount of circular DNA between 24 and 48 h (the period of earliest viral DNA synthesis), and replicate cultures infected in the presence of PAA, cycloheximide, and aphidicolin contained similar amounts of early HMW DNA 24 h after infection. For HCMV,

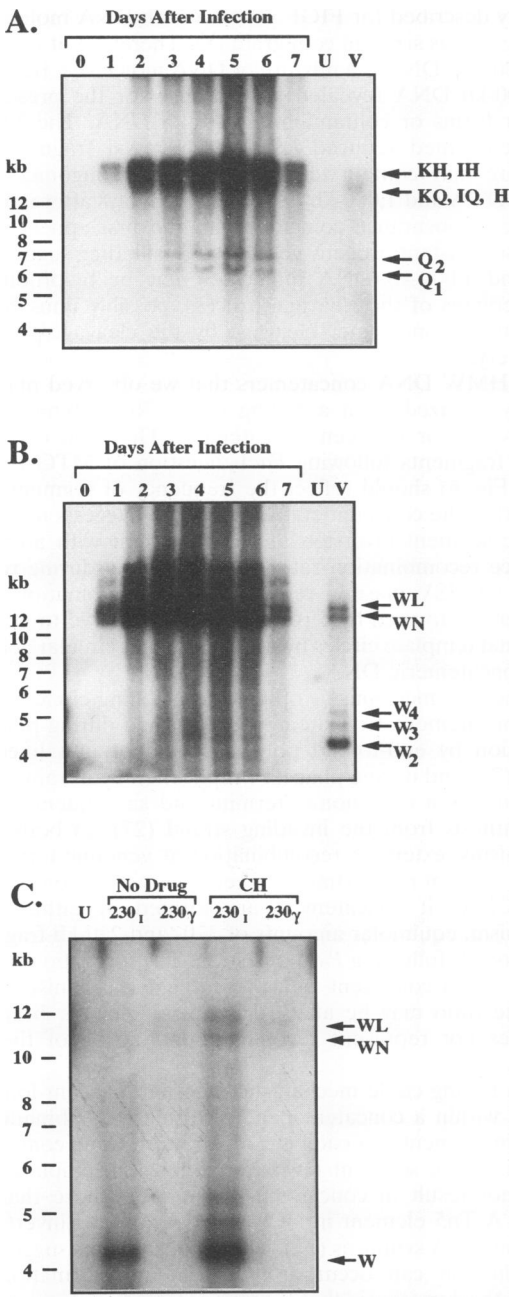

FIG. 11. Terminal fragment analysis of early HMW DNA. HMW DNA was prepared at the times indicated, digested with *Hin*dIII or *Eco*RI, and electrophoresed on 0.6% agarose, and DNA fragments were detected with probes specific for the long- and short-arm termini as in Fig. 5. (A) Hybridization of *Hin*dIII digests with pON2333 to detect short-arm terminal Q fragments. The positions of Q and H terminal fragments and joint fragments KQ, KH, IQ, and IH are indicated. (B) Hybridization of *Eco*RI digests with pON227 to detect long-arm terminal W fragments. The positions of W terminal fragments and joint fragments WN and WL are indicated. In panel A and B, lanes V contain virion DNA and lanes U contain uninfected cell DNA. (C) During the experiment shown in Fig. 10A, replicate DNA samples were separated by FIGE, and both HMW and inoculum 230-kb DNA samples were cut from the gel. The HMW DNA samples were irradiated with 30 kilorads and separated again by FIGE. DNA migrating in the 230-kb range (230_γ DNA) was extracted from the agarose along with the inoculum 230-kb DNA (230_I) prepared from the first separation. These DNAs were digested with *Eco*RI, separated by conventional electrophoresis, and hybridized with pON227 to detect the long-arm terminal fragment W. Lane U contains uninfected cell DNA, and CH indicates DNAs from cycloheximide-treated cultures. The positions of W terminal fragments and joint fragments WN and WL are indicated. Positions of DNA markers are indicated at the left of each gel.

it is therefore unlikely that an early θ replicative stage enhances the circular template copy number prior to the initiation of late HMW DNA synthesis.

Late HMW DNA appears between 20 and 24 h after infection and is made by viral DNA polymerase because its formation is completely inhibited by PAA. The pulse-chase experiments suggest that late HMW DNA is a precursor to progeny genomes, and terminal fragment analysis detected few terminal restriction fragments. HCMV late HMW DNA is therefore analogous to the large replicative DNA observed by sucrose gradient sedimentation of DNA from pseudorabies virus- and HSV-infected cells (4, 16, 18).

HCMV late HMW DNA is not composed of interlocked genome-length circles because irradiation of late HMW DNA generated random fragments but no distinct band of genome-length fragments. Thus, late-stage θ replication with a circular RI is excluded.

To obtain additional evidence that late HMW DNA is concatemeric, we studied the MTO-1 virus. In two different experiments, one in which MTO-1 late HMW DNA was partially digested with *Pac*I and one in which late HMW DNA from a mixed infection was digested, a 460-kb fragment corresponding to two HCMV genome lengths was detected. Furthermore, the differential hybridization of the *Xba*I-E and *Xba*I-S probes indicates that the 370-kb *Pac*I digest product is derived from adjacent genomes with different long-arm orientations. These observations confirm that late HMW DNA is concatemeric. The low levels of the 460-kb dimer and the absence of 690-kb trimers, 920-kb tetramers, etc., may be due to dilution of integer multimers by non-integer-size fragments arising from inversion or due to branching between concatemers arising from intramolecular recombination. The failure of extensive *Pac*I digestion to release all of the HMW DNA from the gel wells (Fig. 6) suggests that branches or some other additional complexity (lariats, etc.) are present in HMW DNA.

Terminal fragment analysis also shows that late HMW DNA is not a catenane of unit circles and suggests a concatemeric structure. Circular DNA should not contain terminal fragments, yet low levels of terminal fragments were present in late HMW DNA. If these terminal fragments were from contamination by linear 230-kb molecules, they should have contributed equal amounts of long- and short-arm termini; however, short-arm terminal fragments were detected in late HMW DNA in the absence of long-arm terminal fragments.

Figure 12 illustrates a possible mechanism to account for the low levels of termini in late HMW DNA and the excess of short-arm termini relative to long-arm termini. In this mechanism, short-arm terminal ends of replicative concatemers are preferentially chosen for insertion into empty capsids. DNA is fed in until one unit genome has entered and is then cleaved to release the genome within the capsid, creating a new short-arm terminus on the concatemer. The newly formed long-arm terminus remains within the capsid and is lost from the concatemeric DNA. A process by which long- and short-arm termini are distinguished during cleavage is probable because multiple *a* sequence reiterations occur at long-arm termini, but short-arm termini either lack an *a* sequence or have only a

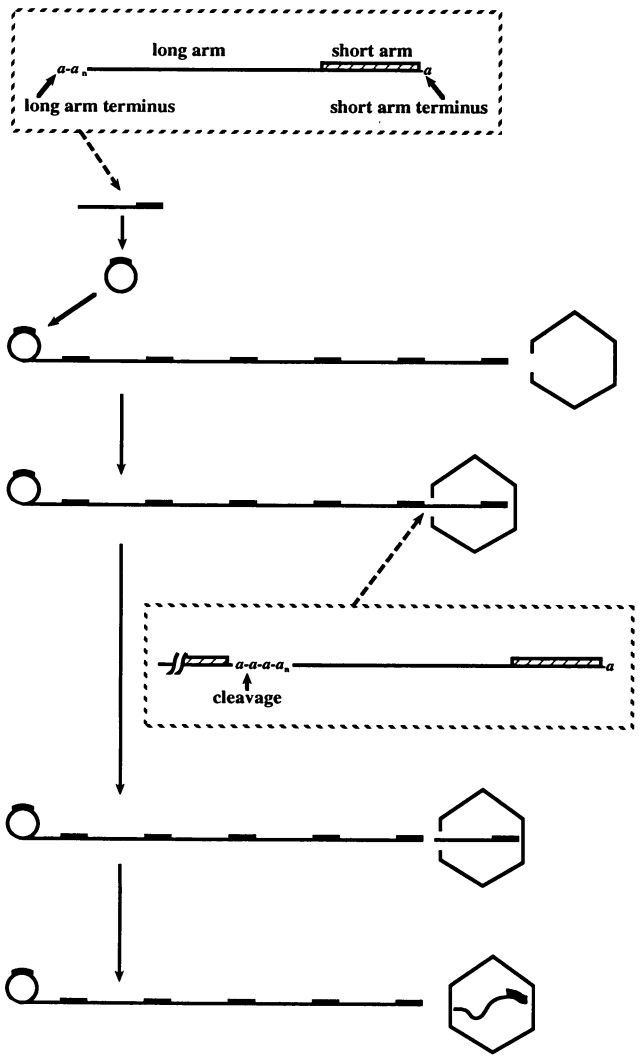

FIG. 12. Model of HCMV DNA replication, insertion, cleavage, and packaging. Unit linear genomic DNA circularizes and replicates by a rolling circle mechanism to form a long linear concatemer. Short-arm termini on RI concatemers are preferentially inserted into empty capsids, and DNA is fed in until a complete genome has entered and the capsid is full. Cleavage occurs between the last two *a* sequences in the reiterated run of *a* sequences located between genomes within the concatemer. The newly created long-arm terminus remains within the capsid, while a new short-arm terminus is created on the concatemer.

single copy (36). We propose that cleavage usually occurs between the last two *a* sequences to enter the capsid, leaving multiple *a* sequences on the long-arm terminus of the newly formed genome.

The origin and function of the 500- and 1,000-kb DNAs are unclear. When 500-kb DNA is separated by FIGE, it contains a 500-kb component and a 230-kb component. The 230-kb component contains normal terminal fragments, indicating that it is not derived from random breakage of 230-kb circles and may simply be contamination by linear 230-kb molecules. The 500-kb DNA is, however, not entirely composed of 230-kb DNA because after a second separation, the 500-kb component is deficient in both termini and is therefore a distinct replicative form.

The 1,000-kb DNA migrates within a region of limited mobility described for FIGE gels in which DNA molecules of heterogeneous size can comigrate (8). Therefore, it is possible that 1,000-kb DNA is a mixture of DNA molecules. Irradiation of 1,000-kb DNA revealed no evidence for the presence of circular forms or contaminating 230-kb DNA. The 1,000-kb DNA contained reduced levels of terminal fragments and therefore may contain tetramers or larger oligomers. Both 500-kb DNA and 1,000-kb DNA appear 3 days after infection, and their appearance coincides with the first appearance of nuclease-resistant progeny genomes. This finding suggests that 500- and 1,000-kb DNA molecules may be by-products or intermediates of the cleavage process, possibly unusable end products of concatemer cleavage by the cleavage/packaging machinery.

The HMW DNA concatemers that we observed may have been synthesized from a rolling circle. Recombination may occur within or between concatemers. The ratio of 370- to 230-kb fragments following *Pac*I digestion of MTO-1 HMW DNA (Fig. 6) should reflect the frequency of segment inversion within the concatemer. The low ratio suggests infrequent genome segment inversion and is consistent with an intra-*a* sequence recombination rate of 8% observed during replication of an HSV plasmid replicon (9). Recombination within concatemers formed by a rolling circle may serve to generate additional template circles by deletion of unit circular genomes from concatemeric DNA.

Replicative mechanisms other than a rolling circle can also form concatemers. Concatemers are formed during phage T7 replication by end-to-end polymerization of unit linear genomes (22) and during phage T4 replication by intramolecular strand invasion of genomic termini and subsequent priming and synthesis from the invading strand (27). In both phage mechanisms, extensive recombination at genomic termini results in random reassortment of genomes within concatemers. For HCMV, if concatemers are formed by either phage mechanism, equimolar amounts of 370- and 230-kb fragments should result following *Pac*I digestion. The low ratio observed (Fig. 6) is not consistent with these phage mechanisms; however, the ratio may be affected by intramolecular branching and does not represent recombination outside of the long repeats.

For a rolling circle mechanism, different adjacent long-arm isomers within a concatemer indicate that recombination resulting in segment inversion occurs after or during concatemer synthesis, since segment inversion within the template circle would not result in concatemers containing more than one isomer. A Tn*5* element in an HSV replicon also inverts only following DNA synthesis (37). These observations suggest that recombination can occur after concatemer formation and support the hypothesis that *a* sequence-mediated recombination is enhanced by strand invasion of free termini created on the ends of concatemers by the cleavage/packaging process (32).

ACKNOWLEDGMENTS

We are grateful to M. Stinski for providing the *Xba*I-E and *Xba*I-S plasmids, H. Browne for providing pATH3ON, J. Pagano for providing the Epstein-Barr virus *Bam*HI W plasmid, and E. Mocarski for providing pON227 and pON2333 and for advice and protocols for preparing and transfecting HCMV DNA.

REFERENCES

1. **Adler, S. P.** 1985. The molecular epidemiology of cytomegalovirus transmission among children attending a day care center. J. Infect. Dis. **152**:760–768.
2. **Adler, S. P.** 1986. The molecular epidemiology of cytomegalovirus:

evidence for viral transmission to parents from children infected at a day care center. Pediatr. Infect. Dis. **5**:315–318.
3. **Anders, D. G., and S. M. Punturieri.** 1991. Multicomponent origin of cytomegalovirus lytic-phase DNA replication. J. Virol. **65**:931–937.
4. **Ben-Porat, T., A. S. Kaplan, B. Stehn, and A. S. Rubenstein.** 1976. Concatemeric forms of intracellular herpesvirus DNA. Virology **69**:547–560.
5. **Ben-Porat, T., F. J. Rixon, and M. L. Blankenship.** 1979. Analysis of the structure of pseudorabies virus. Virology **95**:285–294.
6. **Ben-Porat, T., and R. A. Veach.** 1980. Origin of replication of the DNA of a herpesvirus (pseudorabies). Proc. Natl. Acad. Sci. USA **77**:172–175.
7. **Ben-Porat, T.** 1983. Replication of herpesvirus DNA, p. 81–106. *In* B. Roizman (ed.), The herpesviruses, vol. I. Plenum Press, New York.
8. **Carle, G. F.** 1992. Field-inversion gel electrophoresis, p. 3–18. *In* M. Burmeister and L. Ulanovsky (ed.), Methods in molecular biology, vol. 12. Pulsed-field gel electrophoresis. Humana Press, Totowa, N.J.
9. **Dutch, R. E., R. C. Bruckner, E. S. Mocarski, and I. R. Lehman.** 1992. Herpes simplex virus type 1 recombination: role of DNA replication and viral *a* sequences. J. Virol. **66**:277–285.
10. **Fayez, M., P. Hamzeh, S. Lietman, W. Gibson, and G. S. Hayward.** 1990. Identification of the lytic origin of DNA replication of human cytomegalovirus by a novel approach utilizing gancyclovir-induced chain termination. J. Virol. **64**:6184–6195.
11. **Friedmann, A., and Y. Becker.** 1977. Circular and circular-linear DNA molecules of herpes simplex virus. J. Gen. Virol. **37**:205–208.
12. **Friedmann, A., J. Shlomai, and Y. Becker.** 1977. Electron microscopy of herpes simplex virus DNA molecules isolated from infected cells by centrifugation in $CsCl_2$ density gradients. J. Gen. Virol. **34**:507–522.
13. **Garber, D., S. Beverley, and D. Coen.** 1993. Demonstration of circularization of herpes simplex virus DNA following infection using pulsed field gel electrophoresis. Virology **197**:459–462.
14. **Geelen, J., and M. Weststrate.** 1981. Organization of the human cytomegalovirus genome, p. 325–343. *In* Y. Becker (ed.), Herpesvirus DNA. Martinus Nijhoff Publishers, The Hague.
15. **Hirsch, I., G. Cabral, M. Patterson, and N. Biswal.** 1977. Studies on the intracellular replicating DNA of herpes simplex virus type 1. Virology **81**:48–61.
16. **Hirsch, I., J. Roubal, and V. Vonka.** 1976. Replicating DNA of herpes simplex virus type 1. Intervirology **7**:155–175.
17. **Jacob, R. J., L. S. Morse, and B. Roizman.** 1979. Anatomy of herpes simplex virus DNA. XII. Accumulation of head-to-tail concatemers in nuclei of infected cells and their role in the generation of the four isomeric arrangements of viral DNA. J. Virol. **29**:448–457.
18. **Jacob, R. J., and B. Roizman.** 1977. Anatomy of herpes simplex virus DNA. VIII. Properties of the replicating DNA. J. Virol. **23**:394–411.
19. **Jean, J., and T. Ben-Porat.** 1976. Appearance *in vivo* of single-stranded complementary ends on parental herpesvirus DNA. Proc. Natl. Acad. Sci. USA **73**:2674–2678.
20. **Jean, J., M. L. Blankenship, and T. Ben-Porat.** 1977. Replication of herpesvirus DNA. I. Electron microscopic analysis of replicative structures. Virology **79**:281–291.
21. **Jean, J., N. Yoshimura, T. Furukawa, and S. Plotkin.** 1978. Intracellular forms of the parental human cytomegalovirus genome at early stages of the infective process. Virology **86**:281–286.
22. **Kornberg, A., and T. A. Baker.** 1992. DNA replication, p. 590–597. W. H. Freeman & Co., New York.
23. **Lai, A. C. K., and Y. Chu.** 1991. A rapid method for screening vaccinia virus recombinants. BioTechniques **10**:564–565.
24. **MacGregor, G. R., A. E. Mogg, J. F. Burke, and C. T. Caskey.** 1987. Histochemical staining of clonal mammalian cell lines expressing *E. coli* β-galactosidase indicates heterogeneous expression of the bacterial gene. Somatic Cell. Mol. Genet. **13**:253–265.
25. **McGeogh, D. J.** 1987. The genome of herpes simplex virus: structure, replication, and evolution. J. Cell. Sci. Suppl. **7**:67–94.
26. **Mocarski, E. S., and B. Roizman.** 1982. Structure and role of the herpes simplex virus DNA termini in inversion, circularization, and generation of virion DNA. Cell **31**:89–97.
27. **Mosig, G.** 1983. Relationship of T4 DNA replication and recombination, p. 120–130. *In* C. K. Mathews, E. M. Kutter, G. Mosig, and P. B. Berget (ed.), Bacteriophage T4. American Society for Microbiology, Washington, D.C.
28. **Poffenberger, K., and B. Roizman.** 1985. A noninverting genome of a viable herpes simplex virus 1: presence of head-to-tail linkages in packaged genomes and requirements for circularization after infection. J. Virol. **53**:587–595.
29. **Roizman, B., R. J. Jacob, D. M. Knipe, L. S. Morse, and W. T. Ruyechgan.** 1979. On the structure, functional equivalence, and replication of the four arrangements of herpes simplex virus DNA. Cold Spring Harbor Symp. Quant. Biol. **43**:809–826.
30. **Roizman, B., and A. Sears.** 1991. Herpes simplex viruses and their replication, p. 849–895. *In* B. N. Fields and D. M. Knipe (ed.), Fundamental virology. Raven Press, New York.
31. **Shlomai, J., A. Friedmann, and Y. Becker.** 1976. Replicative intermediates of herpes simplex virus DNA. Virology **69**:647–659.
32. **Smiley, J. R., J. Duncan, and M. Howes.** 1990. Sequence requirements for DNA rearrangements induced by the terminal repeat of herpes simplex virus 1 KOS DNA. J. Virol. **64**:5036–5050.
33. **Spaete, R. R., and E. S. Mocarski.** 1985. The *a* sequence of the cytomegalovirus genome functions as a cleavage/packaging signal for herpes simplex virus defective genomes. J. Virol. **54**:817–824.
34. **Stinski, M. F.** 1991. Cytomegalovirus and its replication, p. 929–950. *In* B. N. Fields and D. M. Knipe (ed.), Fundamental virology. Raven Press, New York.
35. **Tamashiro, J. C., D. Filpula, T. Friedmann, and D. H. Spector.** 1984. Structure of the heterogeneous L-S junction region of human cytomegalovirus strain AD169 DNA. J. Virol. **52**:541–548.
36. **Tamashiro, J. C., and D. H. Spector.** 1986. Terminal structure and heterogeneity in human cytomegalovirus strain AD169. J. Virol. **59**:591–604.
37. **Weber, P. C., M. D. Challberg, N. J. Nelson, M. Levine, and J. C. Glorioso.** 1988. Inversion events in the HSV-1 genome are directly mediated by the viral DNA replication machinery and lack sequence specificity. Cell **54**:369–381.